J Mater Sci (2008) 43:7313–7319
DOI 10.1007/s10853-008-2964-8

ULTRAFINE-GRAINED MATERIALS

Tailoring structures through two-step annealing process in nanostructured aluminum produced by accumulative roll-bonding

Naoya Kamikawa · Xiaoxu Huang · Niels Hansen

Received: 6 March 2008 / Accepted: 20 August 2008 / Published online: 18 September 2008

Abstract Due to structural and textural heterogeneities and a high content of stored energy, annealing of nanostructured metals is difficult to control in order to avoid non-uniform coarsening and recrystallization. The present research demonstrates a method to homogenize the structure by annealing at low temperature before annealing at high temperature. By this two-step process, the structure is homogenized and the stored energy is reduced significantly during the first annealing step. As an example, high-purity aluminum has been deformed to a total reduction of 98.4% (equivalent strain of 4.8) by accumulative roll-bonding at room temperature. Isochronal annealing for 0.5 h of the deformed samples shows the occurrence of recrystallization at 200 °C and above. However, when introducing an annealing step for 6 h at 175 °C, no significant recrystallization is observed and relatively homogeneous structures are obtained when the samples afterwards are annealed at higher temperatures up to 300 °C. To underpin these observations, the structural evolution has been characterized by transmission electron microscopy, showing that significant annihilation of high-angle boundaries, low-angle dislocation boundaries, and dislocations characterizes the low-temperature annealing step. In a discussion, the observed annealing behavior is related to these structural changes.

N. Kamikawa · X. Huang (✉) · N. Hansen
Center for Fundamental Research: Metal Structures in Four Dimensions, Materials Research Department, Risø National Laboratory for Sustainable Energy, Technical University of Denmark (Risø DTU), 4000 Roskilde, Denmark
e-mail: xiaoxu.huang@risoe.dk

Introduction

Nanostructured metals, which have an average grain size of several hundred nanometer or less, are expected to be advanced structural materials for the next generation because of their excellent mechanical properties. One promising method to produce bulk nanostructured metals is high strain deformation [1–3], and well-developed techniques are high-pressure torsion [2, 4], equal channel angular extrusion/pressing [3, 5, 6], and accumulative roll-bonding (ARB) [7, 8]. In fact, it has experimentally been found that nanostructured metals show a very high strength; typically several times higher than observed in coarse-grained materials, but a limited ductility; only a few percent of uniform elongation [9–15]. For practical application of nanostructured metals, it is therefore required to optimize the balance between the strength and the ductility, and one of the possibilities could be an annealing treatment at a relatively low temperature in order to prevent a significant structural coarsening. In previous studies, the annealing behavior of ultrafine-grained or nanostructured metals has been investigated [16–22], but in most of the cases heterogeneous structural coarsening, i.e., conventional discontinuous recrystallization, takes place after high-temperature annealing [16–18, 21, 22]. Such a discontinuous recrystallization is probably due to a high energy stored in the sample and both microstructural and textural heterogeneities. A detailed and careful structural characterization is therefore required in order to explore the annealing behavior of nanostructured metals. Moreover, an optimization of the annealing conditions is necessary in order to control the structural coarsening which in turn controls the mechanical properties of the metal.

In the present study, a high-purity aluminum deformed to a high strain was used as a starting sample for the

annealing experiments. Deformed samples were isochronally annealed at different temperatures. Samples were also annealed by a two-step method; a first step at a low-temperature, long-time annealing and a second step of high-temperature annealing. The structures of the as-deformed and annealed samples are carefully characterized and a correlation between the structure and the annealing behavior for both methods is discussed. In the following, the investigated samples are in general called nanostructured aluminum. The reason for choosing this term is the structure scale after plastic deformation which is in the nanoscale region (<1 μm).

Experimental

A high-purity aluminum with a purity of 99.99 wt.% (4N–Al) was used for this study. The cast ingot of 4N–Al was cold-rolled to 1 mm thickness and annealed at 350 °C for 0.5 h to obtain a fully recrystallized structure with an average grain size of 41 μm. Sheets with a thickness of 1 mm, a width of 40 mm, and a length of 250 mm were used as a starting material.

The ARB was applied to achieve a high strain deformation. For the detailed ARB procedure in the present study, see [21, 23, 25]. The roll-bonding was carried out at room temperature under a non-lubricated condition of the roll surfaces. The ARB process was repeated up to six cycles, giving a total thickness reduction of 98.4% or an equivalent strain of 4.8.

The 6-cycle ARB samples were isochronally annealed in air for 0.5 h at different temperatures from 100 to 400 °C. This annealing treatment will hereafter be referred to as one-step annealing. The samples were also annealed at 175 °C for 6 h and then annealed at high temperatures from 200 to 600 °C for 0.5 h, referred to as two-step annealing. In all cases, the samples were air-cooled down to room temperature after annealing. In this article, only results for samples annealed up to 300 °C are reported.

The as-deformed and annealed samples were characterized by transmission electron microscopy (TEM) and electron backscatter diffraction (EBSD) in a field emission gun scanning electron microscope (SEM). Longitudinal sections containing the normal direction (ND) and the rolling direction (RD) of the sheets were used for both TEM and EBSD. TEM thin foils and EBSD samples were electropolished by a twin-jet technique. The thin foils were observed in a JEOL JEM-2000FX TEM operated at 200 kV. An online Kikuchi-line analysis technique was used for fine-scale orientation measurement in the TEM [24]. The individual dislocations were observed under multi-beam diffraction conditions and the dislocation density was measured from TEM images where the foil thickness was determined by a convergent beam electron diffraction technique. The EBSD measurement and data analysis were carried out using TSL software in a FEI XL30S SEM or by HKL software in a Zeiss Supra 35 SEM. Boundaries with misorientation angles below 2° were disregarded as being below the angular resolution in the EBSD measurements.

Results

Deformed state

The deformation structure of the 6-cycle ARB sample was characterized by EBSD and TEM. The detailed structural features have previously been reported [23, 25] and are summarized in the following.

Figure 1 is a typical structure of the deformed sample observed in the TEM, containing equiaxed structured regions and lamellar structured regions. The average boundary spacing was determined to be 0.69 μm by the random test line method applied to the TEM images. It was confirmed from orientation measurement by Kikuchi-line analysis in the TEM that the equiaxed crystallites are mainly surrounded by high-angle boundaries and the lamellar crystallites are delineated by low-angle boundaries. Such structural characteristics were also observed by

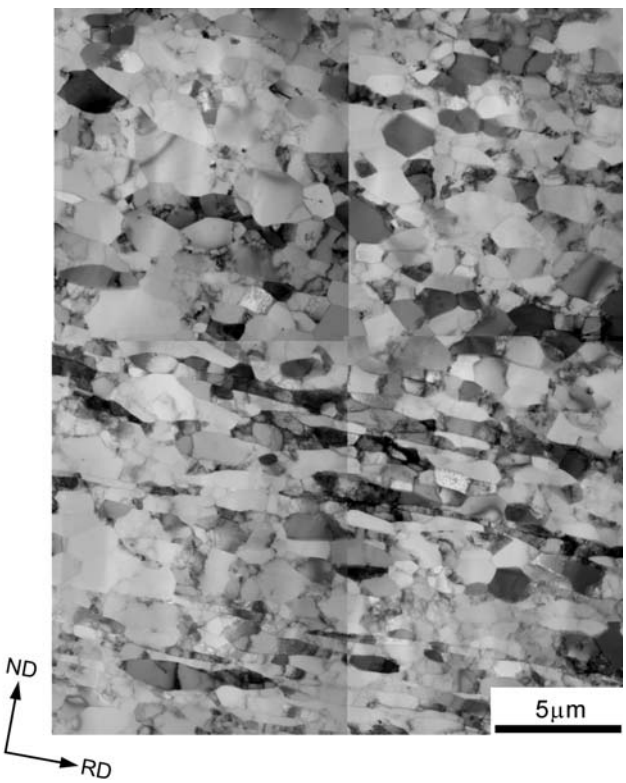

Fig. 1 TEM microstructure of the 6-cycle ARB sample

EBSD [23, 25]. The TEM observation also showed that the equiaxed regions have a lower dislocation density than the lamellar regions. The dislocation density was determined to be 1.01×10^{13} m^{-2} in the equiaxed regions and 3.53×10^{13} m^{-2} in the lamellar regions, giving an average density of 1.23×10^{13} m^{-2} by taking account of the area fraction of each region [23].

The misorientation angle distribution of the boundaries in the sample was analyzed both from the EBSD and TEM results. A good agreement was observed between the EBSD and the TEM results, except that very low-angle boundaries <2° are not included in the EBSD distribution. More than 50% of the boundaries were of high-angle >15°, and at the same time a large number of low-angle boundaries <2° (16.8%) are present, leading to a bimodal misorientation distribution with one peak at small angles and the second peak at misorientation angles around 50°. Such a bimodal misorientation distribution is typical for samples after high strain deformation [26, 27].

Microstructural parameters determined by EBSD and TEM techniques are summarized in Table 1, where. d_t, d_l, and d_R are the boundary spacing measured along the ND, RD and by the linear intercept method, respectively, θ_{av} is the average misorientation angle, f(>15°), f(2–15°), and f(<2°) are the fraction of boundaries with misorientation angle above 15°, between 2 and 15° and below 2°, respectively, and ρ_0 is the dislocation density between the boundaries. Significant differences in the spacing, the misorientation angle, and fraction of the boundaries can be seen between the EBSD and the TEM due to the inclusion of low-angle boundaries (<2°) in the TEM analysis.

Annealed state

One-step annealing

The 6-cycle ARB sample was isochronally annealed for 0.5 h at temperatures from 100 to 300 °C. Figure 2 shows

Table 1 Structural parameters of the 6-cycle ARB and annealed samples

	d_t (μm)	d_l (μm)	d_R (μm)	θ_{av} (°)	f(>15°) (%)	f(2–15°) (%)	f(<2°) (%)	ρ_0 (m^{-2})
As ARB								
EBSD	0.88	1.5	1.1	31.4	72.3	27.7	–	–
TEM	0.57	0.94	0.69	23.6	51.8	31.4	16.8	1.23×10^{13}
ARB + 175 °C 0.5 h								
EBSD	1.2	1.8	1.6	33.7	76.5	23.5	–	–
TEM	0.91	1.2	0.96	22.8	52.8	30.8	16.4	5.98×10^{12}
ARB + 175 °C 6 h								
EBSD	1.9	2.3	2.2	30.1	70.8	29.2	–	–
TEM	2.2	2.3	2.4	33.1	73.7	18.7	7.6	Negligible

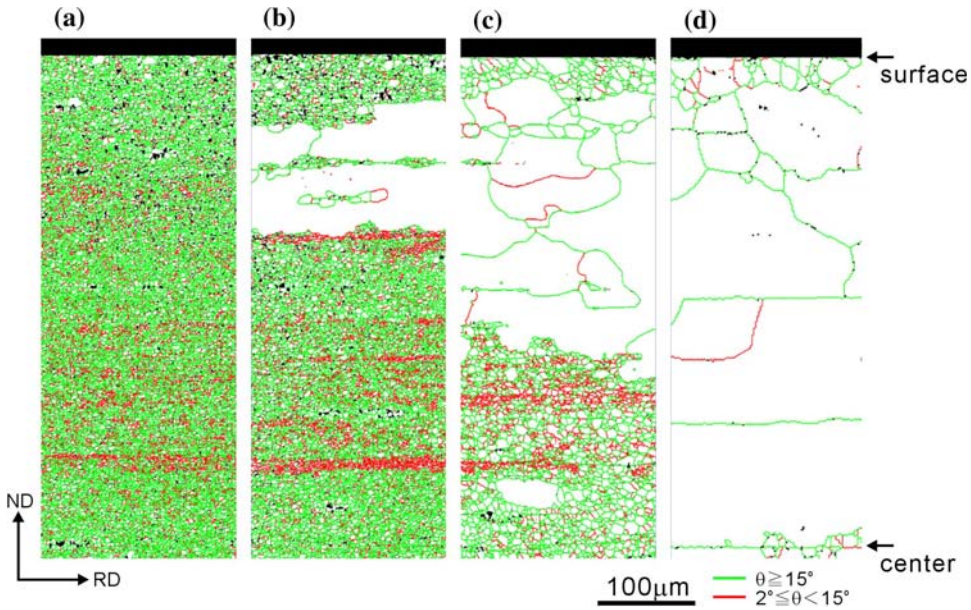

Fig. 2 Boundary maps of the 6-cycle ARB and annealed samples. Annealed at (**a**) 175 °C, (**b**) 200 °C, (**c**) 250 °C, and (**d**) 300 °C for 0.5 h. The measurements were carried out from the thickness center to the surface of the sheets

the through-thickness boundary maps obtained from the EBSD measurement of specimens annealed at different temperatures. By low-temperature annealing at 175 °C and below, the structure gradually coarsened with increasing annealing temperature, but the structure remained relatively homogeneous through the thickness of the sheet (Fig. 2a). At 200 °C, however, recrystallization starts, resulting in a quite heterogeneous structure (Fig. 2b). The fraction recrystallized increases with increasing annealing temperature and at 300 °C and above the whole thickness contains recrystallized grains (Fig. 2c–e). The size of the recrystallized grains shows a large scatter, and some of boundaries surrounding the recrystallized grains are elongated parallel to RD. This may be an effect of bonding interfaces where surface contamination or oxide layers introduced during each rolling cycle may pin the boundary migration. A similar characteristic has been observed in samples deformed by ARB and annealed afterwards [18].

The change in the boundary spacing (d_t) during annealing is shown in Fig. 3, based on the EBSD analysis. After annealing at 175 °C, the distribution shows a single-peak. After annealing at 200 °C, a new peak of large recrystallized grains is observed, resulting in a bimodal distribution of boundary spacings. The fraction and the size of the recrystallized grains increase with increasing annealing temperature. This behavior is typical for discontinuous recrystallization.

Recovery annealing at 175 °C for 0.5 and 6 h

In order to avoid the recrystallization and to obtain a homogeneous structural coarsening, annealing at 175 °C was investigated. As shown in the previous section, the as-deformed specimen contains narrowly spaced high-angle boundaries, low-angle boundaries, and individual dislocations between the boundaries, each of which may have a significant contribution to the stored energy which is the driving force for both recovery and recrystallization. It is therefore suggested that decreasing the content of stored energy may increase the thermal stability of the deformed material. A long-time recovery annealing was therefore introduced. In the present study, an annealing treatment of 175 °C for 6 h is proposed as a first trial. The reason for choosing this temperature is because it is the highest temperature at which no recrystallization took place in the one-step annealing experiment (see Fig. 2a).

Figure 4 shows the TEM structure of the 175 °C/6 h annealed sample. Compared with the as-deformed sample (Fig. 1), a significant structural coarsening can be seen after annealing. The random test line spacing in TEM was measured to be 2.4 μm. There are two different regions observed in the structure; a coarse-grained and a slightly finer-grained regions. Misorientation measurements showed that the

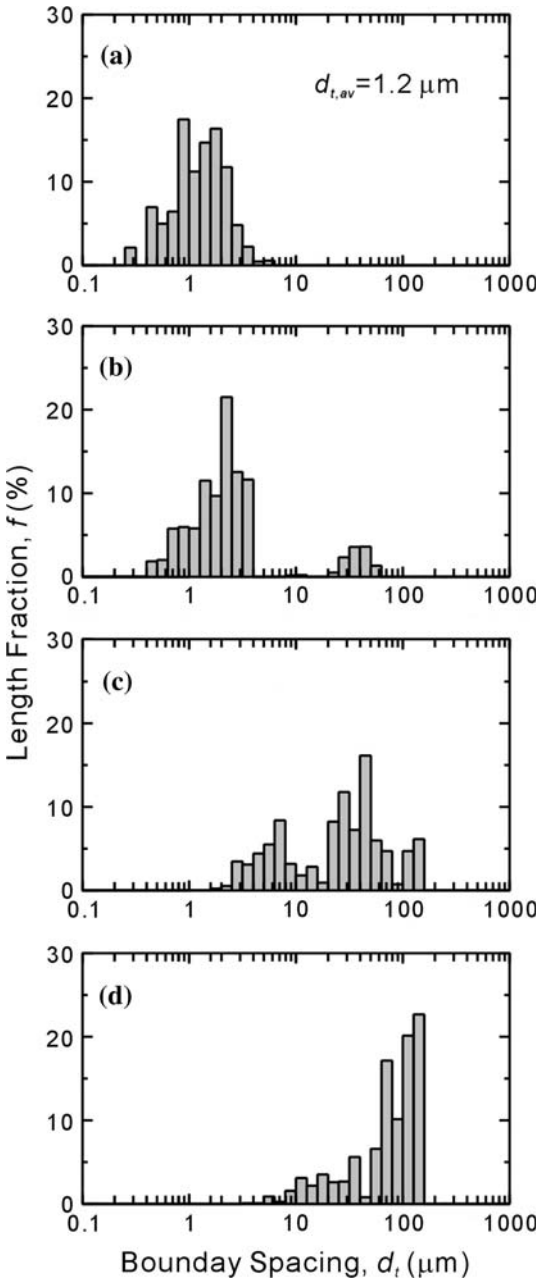

Fig. 3 Distributions of the boundary spacing in the 6-cycle ARB and annealed samples. Annealed at (**a**) 175 °C, (**b**) 200 °C, (**c**) 250 °C, and (**d**) 300 °C for 0.5 h

coarse-grained region consists mainly of high-angle boundaries and the finer-grained region is composed of low-angle boundaries. It is therefore suggested that the coarse- and finer-grained regions in the annealed state originate from the equiaxed and lamellar regions in the as-deformed state, respectively. A comparison of TEM images between the as-deformed and the annealed samples also shows a significant decrease in the density of dislocations between the boundaries. It was quite difficult to find individual dislocations within the crystallites even under multi-beam

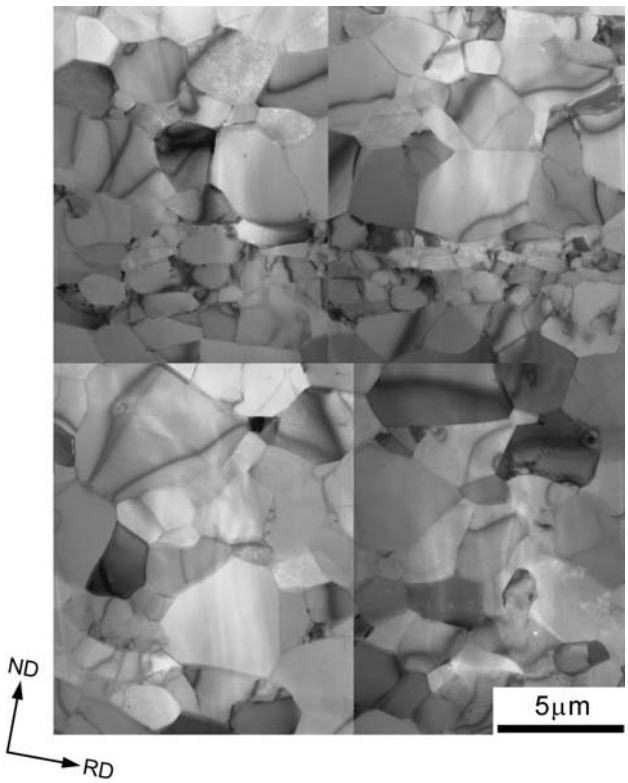

Fig. 4 TEM microstructure of the sample ARB processed and annealed at 175 °C for 6 h

diffraction conditions during the TEM observations, so that it can be assumed that in this sample most of the in-grain dislocations have annealed out.

Structural parameters determined by EBSD and TEM are listed in Table 1, together with the data from the sample annealed at 175 °C for 0.5 h. After annealing at 175 °C for 0.5 h, a slight coarsening and a decrease in the dislocation density are seen but the misorientation angles do not change much. However, after the extended annealing for 6 h, the following structural changes are significant,

(a) a decrease of $f(<2°)$ from 16.8 to 7.6%
(b) a decrease in ρ_0 from 1.2×10^{13} m^{-2} to a negligible number
(c) an increase in d_R from 0.69 to 2.4 μm

As many of the low-angle boundaries have been annealed out there is now a good correspondence between the TEM and the EBSD results.

Two-step annealing

Samples annealed at 175 °C for 6 h have subsequently been annealed at higher temperatures for 0.5 h, which will be referred to as two-step annealing. Figure 5 shows examples of the through-thickness boundary maps obtained from the EBSD measurements for the samples annealed by this two-step method. After the first-step annealing at 175 °C for 6 h (Fig. 5a), a relatively uniform microstructure is observed through the thickness, although some large grains can be seen near the surface. By the second-step annealing at high temperatures, the structural coarsening gradually proceeds with increasing annealing temperature but the homogeneity of the structure is maintained. The change in the distribution of boundary spacings during the two-step annealing is shown in Fig. 6. This figure shows that a fairly uniform coarsening takes place when raising the annealing temperature to 200 and 300 °C.

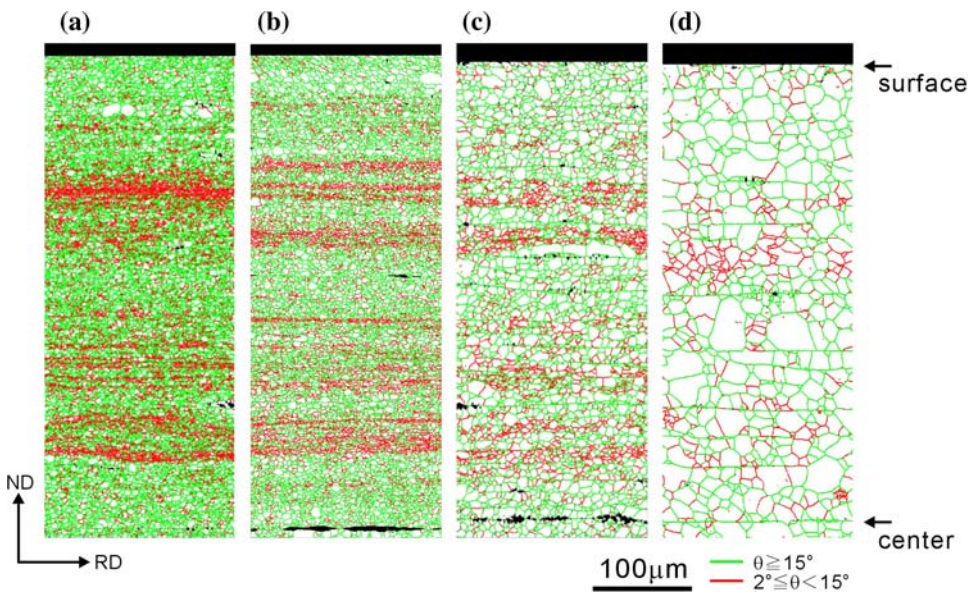

Fig. 5 Boundary maps of the 6-cycle ARB and annealed samples. Annealed at (**a**) 175 °C 6 h, (**b**) 175 °C 6 h + 200 °C 0.5 h, (**c**) 175 °C 6 h + 250 °C 0.5 h, and (**d**) 175 °C 6 h + 300 °C 0.5 h. The measurements were carried out from the thickness center to the surface of the sheets

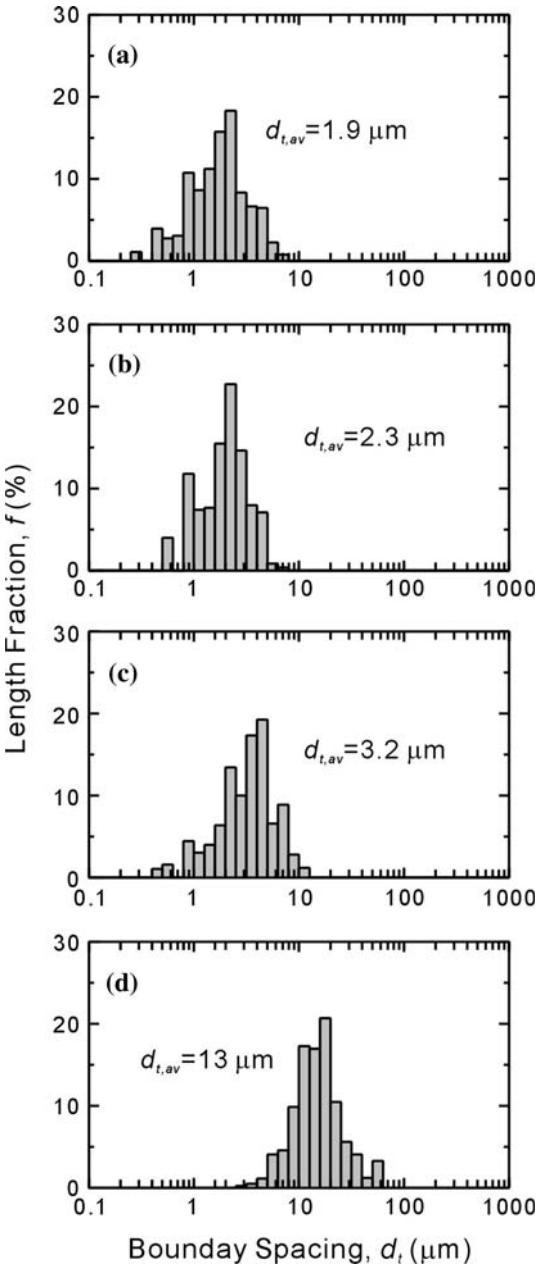

Fig. 6 Distributions of the boundary spacing in the 6-cycle ARB and annealed samples. Annealed at (**a**) 175 °C 6 h, (**b**) 175 °C 6 h + 200 °C 0.5 h, (**c**) 175 °C 6 h + 250 °C 0.5 h, and (**d**) 175 °C 6 h + 300 °C 0.5 h

Discussion

The present study shows that an isochronal annealing for 0.5 h leads to the onset of recrystallization at 200 °C and above, resulting in a quite heterogeneous microstructure. This agrees with previous studies of the annealing behaviors of metals deformed to high strains [16–18, 21, 22]. Because of a very fine-scale boundary spacing and a high density of dislocations, a sample deformed to a high strain stores a large amount of energy, and at the same time the structure can be very heterogeneous [25]. This may lead to the onset of discontinuous recrystallization which takes place heterogeneously as observed. Based on these observations it was suggested that a reduction of stored energy may be effective in retarding the recrystallization and may lead to a homogenization of the annealed structure.

In this study, a two-step annealing, low-temperature for long time (the first step) and a subsequent high-temperature annealing (the second step) has been carried out to explore this suggestion. Figure 5 shows the success of this two-step annealing in suppressing recrystallization and homogenizing the annealed structure. The result clearly showed that the early recrystallization observed at 200 °C (Fig. 2) can be avoided by the two-step annealing and that a fairly uniform structure is present after annealing at 300 °C (Fig. 5). A quantification of the structure of the as-deformed sample and the sample annealed at 175 °C for 6 h showed a significant increase in the boundary spacing and a decrease in the dislocation density between the boundaries (see Table 1). It follows that the annealing for 6 h leads to a significant decrease in the stored energy, i.e., in the driving force for boundary migration during recovery and recrystallization. It is also observed that the long annealing time at 175 °C homogenized the microstructure (see Fig. 5) and significantly decreased the fraction of low- and medium-angle boundaries (see Table 1), which have a lower mobility than high-angle boundaries [28]. Therefore, the average boundary mobility of total boundaries in the annealed state should be higher than that in the as-deformed state. However, the result observed showed a delayed recrystallization, indicating that a significant decrease in the stored energy rather than the increase in mobility is more responsible for the uniform structural coarsening by tow-step annealing. A detailed analysis of the underlying processes is part of the ongoing research, also including annealing of temperature above 300 °C.

In addition to the different causes for a change in the structural stability during annealing, it has been suggested [29–32] that the thermal stability is enhanced in heavily deformed metals when annealed due to a transition from non-equilibrium grain boundaries with high mobility to equilibrium grain boundaries with low mobility. This suggestion is at present hypothetical and needs validation which is outside the scope of the present research.

Another interesting phenomenon observed in the present study is a significant annihilation of loose dislocations as well as low-angle boundaries after the recovery annealing at 175 °C for 6 h. The mechanisms of such an enhanced recovery should be investigated, but as a hypothesis it is suggested that the annihilation rate of loose dislocation and low-angle boundaries increases with an increase in fraction of high-angle boundaries. High-angle boundaries may act

as dislocation sinks and such an effect may be more pronounced in a nanostructured metal since the spacing of high-angle boundaries is small. In Fig. 1, two distinct structures have been observed in the as-deformed sample; an equiaxed structure with a high concentration of high-angle boundaries and a lamellar structure with a high concentration of low-angle boundaries, and the dislocation density between the boundaries was lower in the equiaxed structure than in the lamellar structure. This observation supports the hypothesis of enhanced recovery in nanostructured metals processed by plastic deformation [33].

Conclusions

(1) Short-term annealing for 0.5 h at 200 °C and higher temperatures of a high-purity aluminum deformed to a strain of 4.8 by ARB leads to discontinuous recrystallization.
(2) Extending a recovery heat treatment at 175 °C from 0.5 to 6 h leads to significant structural changes such as a significant decrease in the density of dislocations stored in low-angle boundaries and between the boundaries. Some structural coarsening is observed.
(3) A heat treatment at 175 °C for 6 h recovers and homogenizes the structure in such a way that annealing at higher temperatures up to 300 °C results in uniform annealed structures with a boundary spacing which increases with the annealing temperature.

Acknowledgements The authors gratefully acknowledge the Danish National Research Foundation for supporting the Center for Fundamental Research: Metal Structures in Four Dimension, within which this work was performed. The authors also thank Prof. B. Ralph for useful comments and language correction.

References

1. Altan BS, Miskioglu I, Purcek G, Mulyukov RR, Artan R (2006) Severe plastic deformation: towards bulk production of nanostructured materials. NOVA Science Publishers, New York
2. Valiev RZ, Islamgaliev RK, Alexandrov IV (2000) Prog Mater Sci 45:103. doi:10.1016/S0079-6425(99)00007-9
3. Valiev RZ, Langdon TG (2006) Prog Mater Sci 51:881. doi:10.1016/j.pmatsci.2006.02.003
4. Horita Z et al (1996) J Mater Res 11:1880. doi:10.1557/JMR.1996.0239
5. Segal VM (1995) Mater Sci Eng A 197:157. doi:10.1016/0921-5093(95)09705-8
6. Iwahashi Y, Wang J, Horita Z, Nemoto M, Langdon TG (1996) Scr Mater 35:143. doi:10.1016/1359-6462(96)00107-8
7. Saito Y, Utsunomiya H, Tsuji N, Sakai T (1999) Acta Mater 47:579. doi:10.1016/S1359-6454(98)00365-6
8. Tsuji N, Kamikawa N, Kim HW, Minamino Y (2004) Ultrafine grained materials III. TMS, Ohio, p 219
9. Meyers MA, Mishra A, Benson DJ (2006) Prog Mater Sci 51:427. doi:10.1016/j.pmatsci.2005.08.003
10. Tsuji N, Ito Y, Saito Y, Minamino Y (2002) Scr Mater 47:893. doi:10.1016/S1359-6462(02)00282-8
11. Li BL, Godfrey A, Meng QC, Liu Q, Hansen N (2004) Acta Mater 52:1069. doi:10.1016/j.actamat.2003.10.040
12. Wang YM et al (2004) Scr Mater 51:1023. doi:10.1016/j.scriptamat.2004.08.015
13. Yu CY, Kao PW, Chang CP (2005) Acta Mater 53:4019. doi:10.1016/j.actamat.2005.05.005
14. Xing ZP, Kang SB, Kim HW (2002) J Mater Sci 37:717. doi:10.1023/A:1013879528697
15. Terada D, Inoue S, Tsuji N (2007) J Mater Sci 42:1673. doi:10.1007/s10853-006-0909-7
16. Wang J et al (1996) Acta Mater 44:2973. doi:10.1016/1359-6454(95)00395-9
17. Hasegawa H et al (1999) Mater Sci Eng A 265:188. doi:10.1016/S0921-5093(98)01136-8
18. Cao WQ, Godfrey A, Hansen N, Liu Q, Metall Mater Trans, accepted for publication
19. Prangnell PB, Hayes JS, Bowen JR, Apps PJ, Bate PS (2004) Acta Mater 52:3193. doi:10.1016/j.actamat.2004.03.019
20. Jazaeri H, Humphreys FJ (2004) Acta Mater 52:3251. doi:10.1016/j.actamat.2004.03.031
21. Kamikawa N, Tsuji N, Huang X, Hansen N (2006) Acta Mater 54:3055. doi:10.1016/j.actamat.2006.02.046
22. Li XL, Liu W, Godfrey A, Juul Jensen D, Liu Q (2007) Acta Mater 55:3531. doi:10.1016/j.actamat.2007.02.005
23. Kamikawa N, Tsuji N, Huang X, Hansen N, Minamino Y (2006) Mater Sci Forum 512:91
24. Liu Q (1994) J Appl Cryst 27:755. doi:10.1107/S0021889894002062
25. Kamikawa N, Tsuji N, Huang X, Hansen N (2007) Mater Trans 48:1978. doi:10.2320/matertrans.MA200702
26. Hughes DA, Hansen N (2000) Acta Mater 48:2985. doi:10.1016/S1359-6454(00)00082-3
27. Liu Q, Huang X, Lloyd DJ, Hansen N (2002) Acta Mater 50:3789. doi:10.1016/S1359-6454(02)00174-X
28. Humphreys FJ, Hatherly M (1995) Recrystallization and related annealing behavior. Pergamon, New York
29. Nazarov AA, Romanov AE, Valiev RZ (1993) Acta Metall Mater 41:1033. doi:10.1016/0956-7151(93)90152-I
30. Lian J, Valiev RZ, Baudelet B (1995) Acta Metall Mater 43:4165. doi:10.1016/0956-7151(95)00087-C
31. Horita Z et al (1996) Mater Charact 37:285. doi:10.1016/S1044-5803(96)00178-7
32. Valiev RZ (2003) Adv Eng Mater 5:296. doi:10.1002/adem.200310089
33. Hansen N, Huang X, Møller MG, Godfrey A (2008) J Mater Sci. doi:10.1007/s10853-008-2874-9